

Electrical Conductivity at Surfaces of Silica Nanoparticles with Adsorbed Water at Various Relative Humidities*

Ryosuke Umezawa,[†] Makoto Katsura, and Satoru Nakashima

Department of Earth and Space Science, Graduate School of Science,

Osaka University, Machikaneyama-cho 1-1, Toyonaka, Osaka 560-0043, Japan

(Received 9 January 2018; Accepted 12 August 2018; Published 30 August 2018)

Electrical conductivity of silica nanoparticles deposited on electrodes from colloidal suspension were measured under controlled relative humidity (RH). The electrical conductivity values at 1 kHz increased with increasing RH. Amounts of water adsorbed on silica nanoparticles were measured by quartz crystal microbalance (QCM) and they also increased with increasing RH. An empirical power law relation was observed between the reported surface conductivity and RH data for a silica glass. By applying this relation to the silica nanoparticles, the water film thicknesses are estimated to be from 0.08 nm to 0.23 nm. The corresponding specific surface area (SSA) becomes smaller ($102 \text{ m}^2\text{g}^{-1}$) than the reported value ($215 \text{ m}^2\text{g}^{-1}$), indicating aggregation of the nanoparticles. In fact, aggregated rod-like structures were observed under electron and laser scanning microscopy. The electrical conduction of deposited silica nanoparticles under various RH can be understood by surface conduction in thin water films adsorbed on the nanoparticles. [DOI: 10.1380/ejssnt.2018.376]

Keywords: Amorphous surfaces; Nano-particles; Silicon oxide; Surface conductivity; Water

I. INTRODUCTION

Electrical conduction in insulating or semi-conducting materials under normal environmental ambient conditions is considered to be occurring through adsorbed water on these materials [1–4]. These electrical properties of surfaces became increasingly important in modern material sciences, especially for nanoparticles because of their large surface areas [5, 6]. The electrical conduction on wet surfaces of nanoparticles might lead to undesirable properties of materials in daily use, degradation of materials and their decreasing safety [7].

In the earth's surfaces, rocks and soils above the water table (groundwater) is unsaturated with water inside their pore spaces. In these pores, solid/water/air interfaces are present like the above materials under normal relative humidity (RH) conditions. The electrical conductivity in these unsaturated rocks suggest that surface conductivity changes with decreasing degrees of water saturation and is different from the conductivity in bulk pore water [8]. It should be noted that surface conductivity through wetted mineral grain networks in rocks and soils can be a good measure of water connectivity and material transport properties (permeability, diffusivity) [9, 10].

However, despite several measurements of electrical conductivity on wet material surfaces [1, 2, 11], quantitative understanding of surface conductivity has not been obtained. In particular, relations of surface conductivity with thicknesses of water film adsorbed on material surfaces have never been investigated.

Electrical conductivity of nanoparticles (silica [12], aluminum oxide [5]) have been measured in aqueous solutions, but surface conductivity cannot be evaluated in the presence of bulk water. Electrical conductivity of silica gel [13], silica glass [11], silica monolith [14], TiO₂ nanoparticles [3] and cellulose [15] have been measured

under various RH conditions. Among them, Soffer and Folman (1966) [11] measured surface conductivity of a porous silica glass (Vycor glass) under different water vapor pressures. They observed increasing surface conductivity values with increasing water vapor pressure (RH).

On the other hand, Asay and Kim (2005) [16] examined adsorbed water layers on silicon oxide with increasing RH at room temperature by attenuated total reflection infrared (ATR-IR) spectroscopy. They evaluated water film thicknesses of 0.2 nm to 3 nm corresponding to 1 to 10 water molecular layers at RH values from 7.3% to 99.4%. Torun *et al.* (2014) [17] evaluated water adsorption to silica nanoparticles by FTIR combined with quartz crystal microbalance (QCM). They found adsorption of one monolayer of water on silica at low RH and oriented two monolayers of water at high RH leading to the formation of capillary bridge. Zornoza-Indart and Lopez-Arce (2016) [18] used colloidal silica nanoparticles in consolidation of historical heritage stones by means of agglomeration of spherical silica nanoparticles. However, electrical conductivity measurements have not been conducted in relation to adsorbed water on silica surfaces.

Therefore, in this study, both electrical conductivity and water adsorption amounts have been measured under varying RH conditions on silica. Since only very small amounts of water are adsorbed on flat silica surfaces such as quartz with small surface area, silica nanoparticles are used in this study having large surface area to enable meaningful measurements of both electrical conductivity and adsorbed water. For precise measurements of small amounts of adsorbed water, quartz crystal microbalance (QCM) method [19] was employed here.

II. EXPERIMENTAL

A. Silica nanoparticles

A commercially available colloidal silica nanoparticle suspension (Ludox LS, Sigma-Aldrich), which has been studied by Hamamoto *et al.* (2015) [20], was employed here. The original suspension has 30 wt% of silica parti-

* This paper was presented at the 8th International Symposium on Surface Science, Tsukuba International Congress Center, Tsukuba, Japan, October 22-26, 2017.

[†] Corresponding author: rumezawa@ess.sci.osaka-u.ac.jp

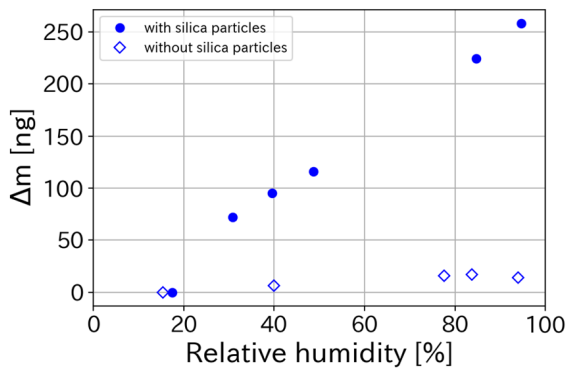


FIG. 2. Weight changes of adsorbed water on silica particles (filled circle) and on the sample-free QCM sensor (open diamond) plotted against relative humidity (RH).

impedance, and is expressed as:

$$Y = \frac{1}{Z}. \quad (3)$$

The complex conductivity σ^* (S m^{-1}) can be calculated from Y :

$$\sigma^* = \sigma' + i\sigma'' = Y \frac{l}{A}, \quad (4)$$

where l is the length between the electrodes and A is the cross-sectional area of the sample. In this study, $l = 0.5$ mm by the micrometer displacement and $A = 1.96 \times 10^{-5}$ m^2 for the circular electrode with 2.5 mm radius.

III. RESULTS

A. Changes in weights by QCM

Weight changes of the adsorbed water on the silica nanoparticles were obtained from resonant frequency shifts by Sauerbrey's equation (Eq. 1) (Table I). Figure 2 shows the weight changes (Δm) against RH values. Δm values of the sample-free QCM sensor (open diamond in

TABLE I. Changes in resonant frequency (ΔF) and weights (Δm) by QCM measurements and conductivity values (σ') at 1 kHz by electrical measurements at various RH values. N/A = not available.

RH (%)	QCM		σ' (S m^{-1}) at 1 kHz
	ΔF (Hz)	Δm (ng)	
17.4	0	0	3.9×10^{-6}
30.8	-67	72	N/A
39.5	-89	96	2.4×10^{-5}
48.7	-108	116	7.0×10^{-5}
60.0	N/A	N/A	2.8×10^{-4}
77.8	N/A	N/A	3.2×10^{-3}
84.7	-209	224	5.3×10^{-3}
94.6	-241	259	7.5×10^{-3}

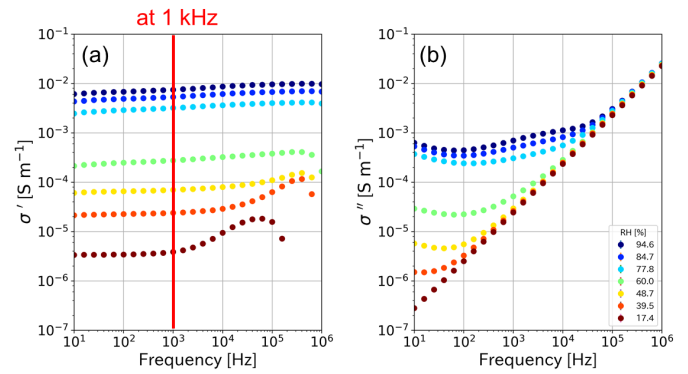


FIG. 3. (a) Real (σ') and (b) imaginary (σ'') parts of electrical conductivity of silica nanoparticles as a function of electrical frequency. The data with increasing RH are shown in different colors from red (RH = 17.4%) to blue (RH = 94.6%). σ' values at 1 kHz are used for further analyses.

Fig. 2) are less than 17 ng. This background water adsorption on the QCM sensor is less than 8% of the weight changes on silica particles. Therefore, Δm values of the QCM sensor with silica particles (filled circle) are considered to be mainly by water adsorption to the silica particles. With increasing RH, about 70 ng to 260 ng of water was adsorbed on the silica nanoparticles.

B. Electrical conductivity of silica particles

Complex conductivity values of silica particles with various RH are plotted against frequency from 10 Hz to 1 MHz (Fig. 3). The data with increasing RH are shown in different colors from red (RH = 17.4%) to blue (RH = 94.6%). The real part of conductivity (σ') increases with increasing RH and becomes relatively constant for frequencies lower than 1 kHz. The imaginary part of conductivity (σ'') also increases with increasing RH at lower frequencies. It increases with frequency.

Since the imaginary part of conductivity (σ'') reflects electrical capacitance of silica nanoparticles, we will use the real part of conductivity (σ') at 1 kHz for further analyses as representative values showing systematic changes with RH. It should be noted that these values are mostly

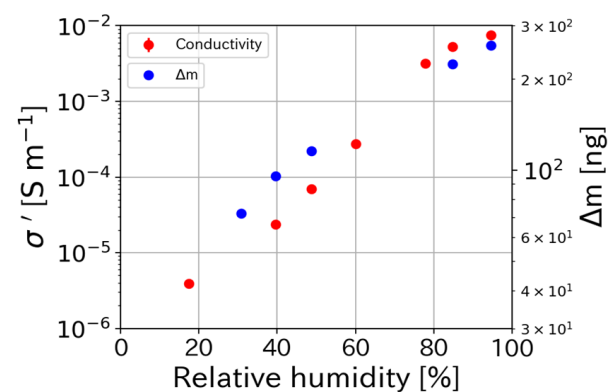


FIG. 4. The real part σ' (red circle) at 1 kHz of electrical conductivity and weight changes Δm (blue circle) for silica nanoparticles against RH in semi logarithmic plots.

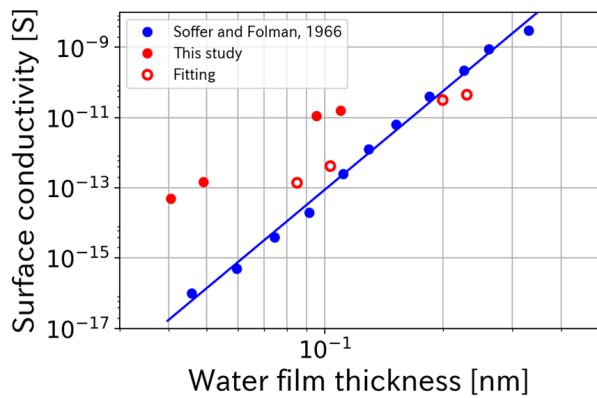


FIG. 5. Surface conductivity of silica nanoparticles at 1 kHz (red filled circle with $SSA = 215 \text{ m}^2\text{g}^{-1}$) and a silica glass (Vycor glass) from Soffer and Folman, 1966 (blue filled circle) are plotted against their water film thicknesses. The data for the silica glass can be fitted by a power law (Eq. 7). The silica nanoparticles data are fitted to the power law relation (red open circle) yielding smaller SSA value ($102 \text{ m}^2\text{g}^{-1}$) and larger water film thickness.

similar from 1 kHz to 10 Hz.

Figure 4 shows the real part of conductivity (σ') at 1 kHz against RH together with adsorbed water weights (Δm). Both σ' and Δm values increase with increasing RH in semi-logarithmic scales.

IV. DISCUSSION

A. Water film thickness adsorbed on silica nanoparticles by using surface area

Weight changes Δm at various RH conditions can be converted to water film thickness h (m) using specific surface area of silica particles SSA_{si} (m^2g^{-1}), density of water ($\rho_w = 998 \text{ kg m}^{-3}$) and weight of silica particles dropped on QCM sensor ($m_{\text{si}} = 11 \mu\text{g}$) by the following equation:

$$h = \frac{\Delta m}{\rho_w SSA_{\text{si}} m_{\text{si}}}. \quad (5)$$

The results of the water film thickness at various RH by using the reported specific surface area of silica particles ($SSA_{\text{si}} = 215 \text{ m}^2\text{g}^{-1}$) are calculated to be less than 0.11 nm. They are plotted with corresponding electrical conductivity values at the same RH conditions (red filled circles in Fig. 5).

Since the van der Waals diameter of water molecules is about 0.282 nm [24], these thicknesses are too small for adsorbed layers of water molecules. In fact, from 0.3 nm to 3 nm of water molecule layers are considered to be adsorbed on silica surfaces at RHs from 7.3% to 99.4% [16]. Therefore, real specific surface area of deposited silica particles on the QCM sensor is considered to be smaller than the specific surface area for separated nanoparticles. The silica particles might be aggregated into some clusters having smaller surface area.

B. Surface conductivity of water film on silica nanoparticles

The surface conductivity Σ_s (S) of silica particles was calculated from the following equation [8]:

$$\Sigma_s = \frac{\sigma' \tau}{\rho SSA_{\text{si}}}, \quad (6)$$

where τ is the tortuosity of surface conduction and ρ is the density of the silica particles ($\rho = 2.2 \times 10^3 \text{ kg m}^{-3}$). The tortuosity of surface conduction τ is assumed here to be 1.

The obtained surface conductivity Σ_s (S) of silica nanoparticles are plotted against the water film thickness calculated from Eq. (5) by using the reported specific surface area ($SSA_{\text{si}} = 215 \text{ m}^2\text{g}^{-1}$) under the same RH (red filled circle in Fig. 5).

Soffer and Folman (1966) [11] reported the d.c. surface conductivity for adsorbed water vapor on a silica glass (Vycor glass). The sample was 20 mm \times 10 mm and 1.25 mm in thickness. Specific surface area is $175 \text{ m}^2\text{g}^{-1}$, as measured by the Ar adsorption Brunauer-Emmett-Teller (BET) method. Water film thickness on the silica glass was calculated here from adsorbed volume of water vapor converted to mass using by the ideal gas law and specific surface area. Obtained surface conductivity and water film thickness for the silica glass are plotted in Fig. 5 (blue filled circle). These data can be empirically fitted by the following power law (blue line):

$$\Sigma_s = 1.8 \times 10^{-4} h^{9.3}. \quad (7)$$

Water film thicknesses on the silica glass and silica nanoparticles are in the similar value ranges. However, the surface conductivity values for silica nanoparticles are larger than those for the silica glass, showing a deviation from the linear trend [Eq. (7)] in Fig. 5.

The larger surface conductivity of silica nanoparticles than the silica glass in Soffer and Folman (1966) can be due to nano-pore structure formation, capillary condensation of water and condensation of dissolved ions such as sodium and sulfate in such pore structure.

By assuming that the surface conductivity of silica nanoparticles is on the empirical power law relation [Eq. (7)] for the silica glass, corresponding specific surface area for silica nanoparticles can be obtained to be $SSA = 102 \text{ m}^2\text{g}^{-1}$ by the least squares fitting of the data (red open circles in Fig. 5). The real specific surface area of deposited silica particles on the QCM sensor can be thus smaller than the reported specific surface area for separated nanoparticles ($SSA_{\text{si}} = 215 \text{ m}^2\text{g}^{-1}$) because of aggregation. The water film thickness for silica nanoparticles becomes larger by this fitting ranging from 0.08 nm to 0.23 nm (red open circles in Fig. 5). Since the water film thickness for silica nanoparticles with the reported SSA_{si} was considered to be too small for adsorbed layers of water molecules, the above new evaluation with smaller SSA might be more realistic.

In order to examine aggregation of samples, Scanning Electron Microscopy equipped with Energy Dispersive X-ray Spectrometer (SEM-EDS) and Laser Scanning Confocal Microscopy (LSCM) observation were performed for

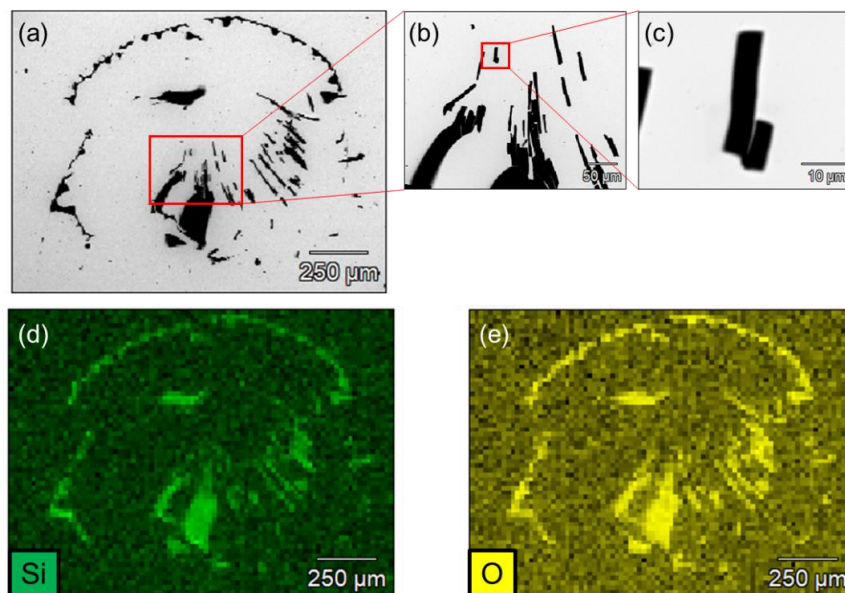


FIG. 6. SEM images of silica nanoparticles. Magnification = (a) $\times 80$, (b) $\times 350$, (c) $\times 3000$. EDS element distribution images of (d) Si and (e) O. They show that silica nanoparticles are aggregated into rod-like structures.

silica nanoparticles deposited on the QCM sensor. SEM observation on silica nanoparticles at magnifications from 80, 350, and 3000 indicate rod-like assembly of silica particles (initial diameter of 12 nm) [Fig. 6(a–c)]. EDS analyses on these particles clearly demonstrated that they are corresponding to silica composed of Si and O [Fig. 6(d, e)].

LSCM observation of the same sample with $\times 10$ objective lens [Fig. 7(a)] show similar aggregated structures of silica nanoparticles to SEM results [Fig. 6(a)]. LSCM observation with $\times 100$ objective lens [Fig. 7(b)] show also the rod-like assembly as in Fig. 6(c). Digital image analyses of these rods indicate that they have widths of several micrometers and heights of several hundred nanometers [Fig. 7(c)].

Although real specific surface area of these rod-like structures with enough spatial resolution could not be evaluated, aggregation of silica nanoparticles (initial diameter of 12 nm) was confirmed both by SEM-EDS and LSCM. This can explain the smaller specific surface area ($SSA = 102 \text{ m}^2\text{g}^{-1}$) estimated from the surface conductivity measurements than that of original separated particles ($SSA_{\text{si}} = 215 \text{ m}^2\text{g}^{-1}$) (Fig. 5).

V. CONCLUSIONS

Electrical conductivity values of silica nanoparticles with adsorbed water were measured under controlled relative humidity (RH). The representative electrical conductivity σ' values at 1 kHz increased with increasing RH. Amounts of water adsorbed on silica nanoparticles were measured by quartz crystal microbalance (QCM). The ad-

sorbed water mass (Δm) values by QCM increased with increasing RH.

The water film thickness h at various RH was first evaluated by using the reported specific surface area of silica nanoparticles ($SSA_{\text{si}} = 215 \text{ m}^2\text{g}^{-1}$). They are calculated to be less than 0.11 nm. The water film thicknesses on a silica glass are evaluated by using the literature data measuring surface conductivities at various RH. These data show an empirical power law (a linear trend) between the surface conductivity and the water film thickness h in a logarithmic plot. By assuming that the surface conductivity of silica nanoparticles is on the same empirical power law relation for the silica glass, corresponding specific surface area for silica nanoparticles can be obtained to be $SSA = 102 \text{ m}^2\text{g}^{-1}$. The real specific surface area of deposited silica particles on the QCM sensor can be thus smaller than the reported specific surface area for separated nanoparticles ($SSA_{\text{si}} = 215 \text{ m}^2\text{g}^{-1}$) because of aggregation. In fact, SEM-EDS and LSCM observations of the sample on the QCM sensor indicated aggregated rod-like structures of silica nanoparticles.

The water film thickness for silica nanoparticles becomes larger by this fitting ranging from 0.08 nm to 0.23 nm, which are more realistic for adsorbed water molecular layers. The electrical conduction of deposited silica particles under various RH conditions can be understood by surface conduction in thin water films adsorbed on the nanoparticles.

ACKNOWLEDGMENTS

RU is supported by Research Assistantship of the Graduate School of Science, Osaka University.

[1] J. H. Anderson and G. A. Parks, *J. Phys. Chem.* **72**, 3662 (1968).

[2] Y. Awakuni and J. H. Calderwood, *J. Phys. D. Appl.*

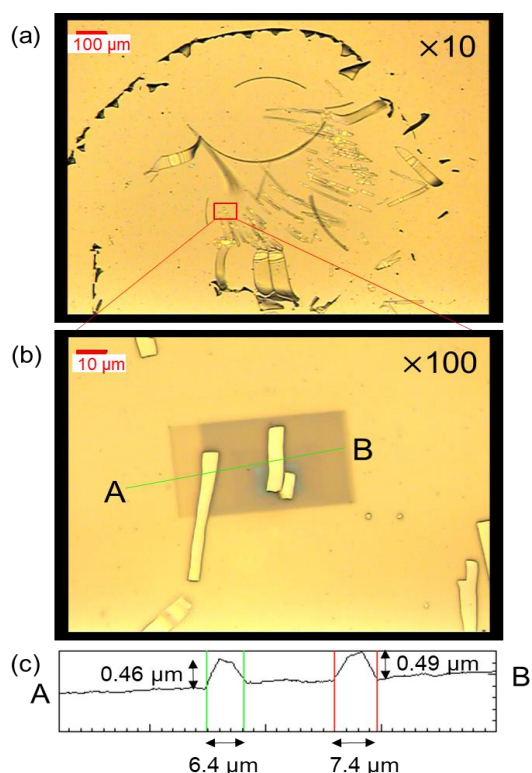


FIG. 7. LSCM images of silica nanoparticles using objective lenses of (a) $\times 10$ and (b) $\times 100$ magnifications. (c) Line profile of the line A–B shown in (b). Rod-like structures have widths of several micrometers and heights of several hundred nanometers. The dark area in (b) corresponds to those observed by SEM due to electron damages.

- Phys. **5**, 1038 (1972).
- [3] M. Usman, K. Rasool, S. S. Batool, Z. Imran, M. Ahmad, H. Jamil, M. A. Rafiq, and M. M. Hasan, *J. Mater. Sci. Technol.* **30**, 748 (2014).
- [4] H. Haspel, G. Peintler, and A. Kukovecz, *Chem. Phys. Lett.* **607**, 1 (2014).
- [5] S. Ganguly, S. Sikdar, and S. Basu, *Powder Technol.* **196**, 326 (2009).
- [6] H. Zhang, A. A. Hassanali, Y. K. Shin, C. Knight, and S. J. Singer, *J. Chem. Phys.* **134**, 024705 (2011).
- [7] J. Wu and A. Schnettler, *IEEE Trans. Dielectr. Electr. Insul.* **15**, 73 (2008).
- [8] R. Umezawa, N. Nishiyama, M. Katsura, and S. Nakashima, *Geophys. J. Int.* **209**, 1287 (2017).
- [9] P. J. Koelemeijer, C. J. Peach, and C. J. Spiers, *J. Geophys. Res. Solid Earth* **117**, 1 (2012).
- [10] C. Mawer, R. Knight, and P. K. Kitanidis, *Water Resour. Res.* **51**, 599 (2014).
- [11] A. Soffer and M. Folman, *Trans. Faraday Soc.* **62**, 3559 (1966).
- [12] Y. Zhao, M. Wang, and R. B. Hammond, *J. Nanosci. Nanotechnol.* **13**, 808 (2013).
- [13] M. T. Colomer and M. A. Anderson, *J. Non-Cryst. Solids* **290**, 93 (2001).
- [14] F. M. Sayler, M. G. Bakker, J. H. Smått, and M. Lindén, *J. Phys. Chem. C* **114**, 8710 (2010).
- [15] M. Nilsson and M. Strømme, *J. Phys. Chem. B* **109**, 5450 (2005).
- [16] D. B. Asay and S. H. Kim, *J. Phys. Chem. B* **109**, 16760 (2005).
- [17] B. Torun, C. Kunze, C. Zhang, T. D. Kühne, and G. Grundmeier, *Phys. Chem. Chem. Phys.* **16**, 7377 (2014).
- [18] A. Zornoza-Indart and P. Lopez-Arce, *J. Cult. Herit.* **18**, 258 (2016).
- [19] S. Kudo, H. Ogawa, E. Yamakita, S. Watanabe, T. Suzuki, and S. Nakashima, *Appl. Spectrosc.* **71**, 1621 (2017).
- [20] M. Hamamoto, M. Katsura, N. Nishiyama, R. Tononue, and S. Nakashima, *e-J. Surf. Sci. Nanotech.* **13**, 301 (2015).
- [21] L. Greenspan, *J. Res. Natl. Bur. Stand. Sect. A Phys. Chem.* **81A**, 89 (1977).
- [22] G. Sauerbrey, *Z. Phys.* **155**, 206 (1959).
- [23] R. Lucklum, C. Behling, R. W. Cernosek, and S. J. Martin, *J. Phys. D: Appl. Phys.* **30**, 346 (1997).
- [24] F. Franks, *Water: A Matrix of Life*, 2nd ed. (Royal Society of Chemistry, Cambridge, 2000).